Domain Wall Conductivity in La-Doped $BiFeO_3$

J. Seidel,[1,2] P. Maksymovych,[3] Y. Batra,[4] A. Katan,[2] S.-Y. Yang,[5] Q. He,[1] A. P. Baddorf,[3] S. V. Kalinin,[3] C.-H. Yang,[6] J.-C. Yang,[7] Y.-H. Chu,[7] E. K. H. Salje,[8] H. Wormeester,[4] M. Salmeron,[2] and R. Ramesh[1,2,5]

[1]*Department of Physics, University of California, Berkeley, California 94720, USA*
[2]*Materials Sciences Division, Lawrence Berkeley National Laboratory, Berkeley, California 94720, USA*
[3]*Center for Nanophase Materials Sciences, Oak Ridge National Laboratory, Oak Ridge, Tennessee 37831, USA*
[4]MESA$^+$ *Research Institute, Universiteit Twente, 7500 AE Enschede, The Netherlands*
[5]*Department of Materials Science and Engineering, University of California, Berkeley, California 94720, USA*
[6]*Department of Physics, Korea Advanced Institute of Science and Technology (KAIST), Daejeon 305-701, Republic of Korea*
[7]*Department of Materials Science and Engineering, National Chiao Tung University, Hsin Chu, Taiwan, Republic of China*
[8]*Department of Earth Sciences, University of Cambridge, Cambridge CB2 3EQ, UK, and Los Alamos National Laboratory, Los Alamos, New Mexico 87544, USA*

(Received 13 May 2010; published 5 November 2010)

The transport physics of domain wall conductivity in La-doped bismuth ferrite ($BiFeO_3$) has been probed using variable temperature conducting atomic force microscopy and piezoresponse force microscopy in samples with arrays of domain walls in the as-grown state. Nanoscale current measurements are investigated as a function of bias and temperature and are shown to be consistent with distinct electronic properties at the domain walls leading to changes in the observed local conductivity. Our observation is well described within a band picture of the observed electronic conduction. Finally, we demonstrate an additional degree of control of the wall conductivity through chemical doping with oxygen vacancies, thus influencing the local conductive state.

DOI: 10.1103/PhysRevLett.105.197603 PACS numbers: 77.80.Fm, 68.37.Ps, 77.80.Dj, 73.61.Le

Understanding and eventually manipulating electronic states in complex oxides is a major goal of contemporary condensed matter physics. Considerable attention is focused on spin-charge-lattice interactions, which provide a mechanism for control of various degrees of freedom, e.g., by applied currents or electric or magnetic fields [1]. Despite this attention, many aspects of these interactions are not fully understood, particularly at interfaces and topological boundaries, such as domain walls, where the same electronic properties are linked to the inherent order parameters of the material, its structure and symmetry [2–6]. Ongoing research is aimed toward a quantitative understanding of how band structure, disorder, and order parameters interact to determine the local conductive state and piezoelectricity in these materials. $BiFeO_3$ (BFO) is a material well known for its dual role as a ferroelectric with high polarization and a canted antiferromagnet with properties that reflect strong spin-lattice interactions [4]. Recently, we reported the possibility of electrical conduction at certain types of domain walls in the multiferroic $BiFeO_3$ system. Such domain patterns (and the accompanying domain walls) were ''written'' using an atomic force microscope. In order to probe the fundamental origins of such conduction phenomena at the domain walls, it is imperative that detailed, statistically averaged transport measurements be carried out on such walls. This is precisely the focus of this paper, in which we investigate the fundamental physics of electrical conductivity at arrays of domain walls in BFO, that were created through careful control of heteroepitaxial boundary conditions [7]. Our temperature dependent measurements reveal a thermally activated transport process that is consistent with the key role of ionized oxygen vacancies in enabling the transport. These results are clearly supported by the observation of a significant enhancement of the transport as a consequence of doping the walls with oxygen vacancies.

100 nm thick La-doped (10%) BFO thin films on $SrRuO_3/DyScO_3$ $(110)_o$ substrates were grown by pulsed laser deposition as reported elsewhere [7]. We chose 10% La doping as this composition allows for ordered stripe domain growth [7]. After deposition the samples were cooled from the deposition temperature ($\sim 650\,^\circ$C) down to room temperature at different oxygen pressures ranging from near atmospheric pressure (500 Torr) over 10 Torr to 100 mTorr. This treatment introduces increasing amounts of oxygen vacancies in the thin film with decreasing oxygen pressure. In all cases atomic force microscopy imaging confirmed the presence of well defined surfaces. X-ray diffraction indicated fully strained epitaxial films and x-ray reflectometry was used to verify film thickness. For our investigation we chose ordered stripe arrays of 109° domain walls, which is one possible wall type in a rhombohedral ferroelectric [8]. The structural width of these domain walls has been shown to be only 1–2 nm from TEM studies [2,9].

We carried out piezoresponse force microscopy (PFM) and conducting atomic force microscopy (*c*-AFM) measurements in ultrahigh vacuum (UHV) environment to investigate the local piezoresponse and conduction

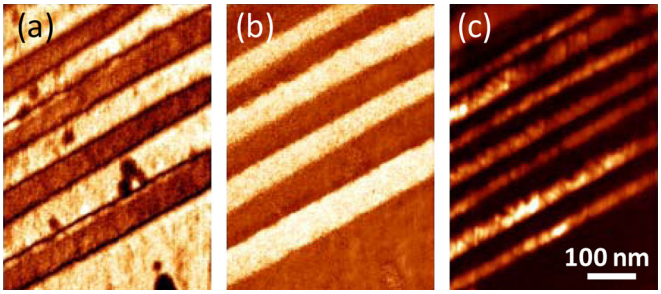

FIG. 1 (color online). (a) PFM amplitude and (b) PFM phase images of a BFO sample with 109° stripe domains. (c) Simultaneously acquired *c*-AFM image of the same area showing that each 109° domain wall is electrically conductive.

properties of these films without interference from surface adsorbates. A visual impression of domain structure and the associated change in local conductivity can be seen in Figs. 1(a)–1(c). Here, a clear correlation of 109° walls in the material and local conductivity indicated by high *c*-AFM currents can be seen [Fig. 1(c)]. The resulting conductive stripes are about 20 nm wide.

In order to characterize the associated piezoelectric properties further, we performed local *I*-*V* measurements using a *c*-AFM based setup in UHV. The acquired data for each *I*-*V* curve give insight into the local conduction mechanism at domain walls in the sample [10,11]. Schottky emission has been shown to be a possible interface limited transport mechanism in ferroelectrics, following

$$I_S = A_{\text{eff}} A T^2 \exp - \left[\frac{\Phi}{k_b T} - \frac{e}{k_b T} \left(\frac{eE}{4\pi\varepsilon\varepsilon_0} \right)^{1/2} \right], \quad (1)$$

where A is the Richardson coefficient, A_{eff} the effective contact area, Φ the Schottky barrier height and ε the dielectric constant, or a modified version of this expression [12,13]. Recently, also tunneling into ferroelectric surfaces was investigated and shown to be dominated by the Fowler-Nordheim mechanism, according to [14]

$$I_{\text{FN}} = A_{\text{eff}} \frac{e^3 m_{Pt}}{8\pi h m_{\text{BFO}} \Phi} E^2 \exp - \left[\frac{8\pi\sqrt{2m_{\text{BFO}}}}{3he} \frac{\Phi^{3/2}}{E} \right], \quad (2)$$

where Φ_B denotes the barrier height, E the electric field, effective A_{eff} tunneling area, and m_{Pt} and m_{BFO} the effective electron mass in the tip and the BFO.

Figure 2 shows local *I*-*V* curves acquired with a conductive AFM tip stepping perpendicular to a domain wall at 340 K. All measurements were done with the same force (load) on the tip to get comparable *I*-*V* curves. Figure 2(b) gives a visual impression of the local conductivity as a function of position across the wall. For Figs. 2(a) and 2(b) the data have been plotted in a way that linearizes them within the framework of a Schottky model. Clearly, for lower current and bias values the data are linear, indicating that Schottky emission is a likely mechanism for the interface limited conduction. For higher currents and biases we see a transition to a significant curvature in the *I*-*V* curves.

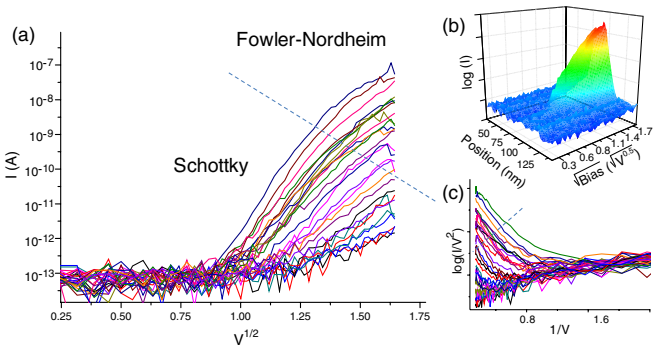

FIG. 2 (color online). (a) Several *I*-*V* curves measured by stepping the c-AFM tip perpendicular across a domain wall at 340 K. Data plotted in linear coordinates for Schottky emission. (b) Typical 3D plot of such a measurement; (c) same data as in (a) plotted in linear coordinates for Fowler-Nordheim tunneling.

If the same data are plotted in a way that linearizes them for Fowler-Nordheim tunneling we see that this high current–high bias region follows straight lines [Fig. 2(c)]. This likely indicates a transition from Schottky emission to Fowler-Nordheim tunneling as the predominant conduction mechanism.

In order to explain the observed behavior of the measured current, we turn to a detailed analysis of the temperature dependent conduction properties at the domain walls, as it is known that domain wall properties are temperature dependent, e.g., for ferroelastic walls in $LaAlO_3$ [15]. For this we performed histogram analysis of *c*-AFM images of conducting walls acquired at different temperatures [Fig. 3(a)]. This allows us to extract spatially averaged current values at each temperature and applied voltage. The current histograms are relatively broad, as disorder may originate from the energy distribution of the oxygen vacancy levels, intrinsic variations in the contact potential, and extrinsic variations in the contact area. The dominant origin will strongly depend on the relative contributions of the surface- and bulk-limited conductance. Temperature dependent current

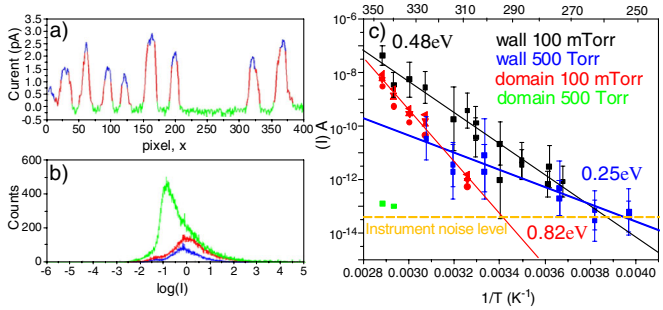

FIG. 3 (color online). (a) Histogram analysis, saturated peak value (blue), whole peak (red), and whole raw data (green) are extracted. (b) Typical histograms of log(*I*). (c) Current levels extracted from histogram analysis of *c*-AFM images at various temperatures and tip biases for the 500 Torr oxygen cooled sample and 100 mTorr oxygen cooled sample. The error bars are FWHM of the corresponding histograms. Activation energies are given in the inset.

values are shown in Fig. 3(c). Activation energies are extracted and shown in the inset.

In all cases, the activation energy for thermally activated transport at the 109° domain walls is extracted to be 0.24–0.5 eV [Fig. 3(a)]. A possible origin for increased activation energies for the 100 mTorr sample could be clustering of vacancies, which has been reported in other materials such as $SrTiO_3$ [16]. There it was shown that oxygen clustering lowers the energy levels of the oxygen vacancies by about a factor of 2. Another possible scenario is that oxygen vacancies directly influence the structure of the domain wall [17–19], thus giving rise to a change in transport properties. We note that similar measurements performed off the domain wall on samples cooled in 100 mTorr oxygen (where overall current values are higher, and thus a reasonable temperature range for *I-V* measurements is accessible) gave consistently higher activation energies of ~0.82 eV [Fig. 3(b)].

The mechanism of the reported transport in La-doped $BiFeO_3$ can be understood by an electronic conduction mechanism as a consequence of oxygen vacancy activation in an electric field. By taking the band gap value, electron affinity, oxygen vacancy band position, and work function of the bulk material and the wall [2,20–22] a schematic of the band structure at the domain wall can be obtained as shown in Fig. 4(a). This model of enhanced conduction at the domain walls, driven by a local change in the band gap, a potential step across the wall as a consequence of the discontinuity in the in-plane component of the polarization and the local defect chemistry is substantiated by the results of experiments in which we deliberately introduced oxygen vacancies into the system by different oxygen cooling pressures during growth. As seen in Fig. 4(b) larger concentrations of oxygen vacancies lead to a correspondingly increased current; changing the cooling pressure from 500 Torr to 100 mTorr leads to an increase in current of more than 1 order of magnitude. Curiously the difference in the activation energy between the domain wall and surface area away from the wall on the 100 mTorr sample is comparable to the predicted lowering of the conduction band edge from DFT calculations (0.2–0.5 V depending on the type of the wall), which may indicate that electrons

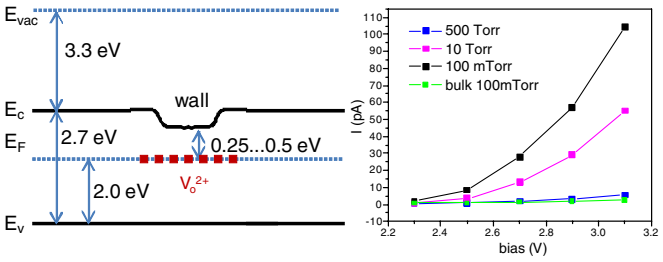

FIG. 4 (color online). (a) Schematic band diagram for the 109° domain wall. (b) Current levels extracted from histogram analysis of *c*-AFM images at room temperature for samples with different oxygen cooling pressure and thus varying density of oxygen vacancies.

tunnel or hop from the tip into the conduction band of $BiFeO_3$, and the corresponding lowering of the band-edge is reflected in the measured barrier height.

In conclusion, we have reported the observation of tunable electronic conductivity at domain walls in La-doped BFO linked to oxygen vacancy concentration. The bias dependence of the domain wall conduction exhibits Schottky emission and Fowler-Nordheim characteristics depending on the current and bias levels. The conductivity is thermally activated with activation energies of $0.24 \ldots 0.5$ eV. From a broader perspective, these results point to the tantalizing possibility of inducing an insulator-metal transition, locally within the confines of the domain wall through careful design of the electronic structure, the state of strain and chemical effects at the domain wall. Further study of correlations between local polarization and conductivity are an exciting approach to understanding the conduction dynamics and associated ferroelectric properties in the presence of strong coupling between electronic conduction and polarization in complex oxides.

This research is supported by the U.S. Department of Energy, Office of Science, under contract No. DE-AC02-05CH1123. A portion of this research was conducted at the Center for Nanophase Materials Sciences, sponsored at Oak Ridge National Laboratory by the Scientific User Facilities Division, U.S. Department of Energy. J. S. acknowledges support from the Alexander von Humboldt Foundation.

[1] J. Heber, Nature (London) **459**, 28 (2009).
[2] J. Seidel *et al.*, Nature Mater. **8**, 229 (2009).
[3] J. Přívratská and V. Janovec, Ferroelectrics **222**, 23 (1999).
[4] E. Salje and H. Zhang, Phase Transit. **82**, 452 (2009).
[5] A. Lubk, S. Gemming, and N. A. Spaldin, Phys. Rev. B **80**, 104110 (2009).
[6] A. Aird and E. K. H. Salje, J. Phys. Condens. Matter **10**, L377 (1998).
[7] Y.-H. Chu *et al.*, Nano Lett. **9**, 1726 (2009).
[8] S. K. Streiffer *et al.*, J. Appl. Phys. **83**, 2742 (1998).
[9] A. Borisevich *et al.*, Nano Lett. (to be published).
[10] P. Maksymovych *et al.*, Nanotechnology (to be published).
[11] J. Simmons, Phys. Rev. **166**, 912 (1968).
[12] J. F. Scott, Chem. Phys. Chem. **10**, 1761 (2009).
[13] Y. Kim *et al.*, Appl. Phys. Lett. **96**, 032904 (2010).
[14] P. Maksymovych *et al.*, Science **324**, 1421 (2009).
[15] J. Chrosch and E. K. H. Salje, J. Appl. Phys. **85**, 722 (1999).
[16] D. D. Cuong *et al.*, Phys. Rev. Lett. **98**, 115503 (2007).
[17] C.-L. Jia *et al.*, Nature Mater. **7**, 57 (2008).
[18] A. Angoshtari and A. Yavari, Comput. Mater. Sci. **48**, 258 (2010).
[19] M. Y. Gureev *et al.*, *18th IEEE International Symposium on the Applications of Ferroelectrics, ISAF 2009* (IEEE, Bellingham, WA, 2009), Vol. 23–27, p. 1.
[20] J. Wu *et al.*, Electrochem. Solid-State Lett. **13**, G9 (2010).
[21] H. Yang *et al.*, Appl. Phys. Lett. **92**, 102113 (2008).
[22] J. Zhang *et al.*, J. Vac. Sci. Technol. B **27**, 2012 (2009).